Supplementary materials

Controlled engineering of $Bi_4O_5Br_2$ and BiOBr via interactions imidazolium ionic liquids and medium during synthesis as a simple method for enhancement of photocatalytic activity

Aleksandra Bielicka-Giełdoń[1], Patrycja Wilczewska[1*], Rafał Ślusarz[1], Artur P. Terzyk[2], Patrycja Parnicka[1], Karol Szczodrowski[3], Jacek Ryl[4], E.M. Siedlecka[1*]

[1]*Faculty of Chemistry, University of Gdansk, Wita Stwosza 63, 80-308 Gdansk, Poland*

[2]*Faculty of Chemistry, Physicochemistry of Carbon Materials Research Group, Nicolaus Copernicus University in Toruń, Jurij Gagarina 7, 87-100 Toruń, Poland*

[3]*Faculty of Mathematics, Physics and Informatics, University of Gdansk, Wita Stwosza 57, 80-308 Gdansk, Poland*

[4]*Institute of Nanotechnology and Materials Engineering, Faculty of Applied Physics and Mathematics, Gdansk University of Technology, Gabriela Narutowicza 11/12, 80-233 Gdansk, Poland*

**corresponding author*

Contents:

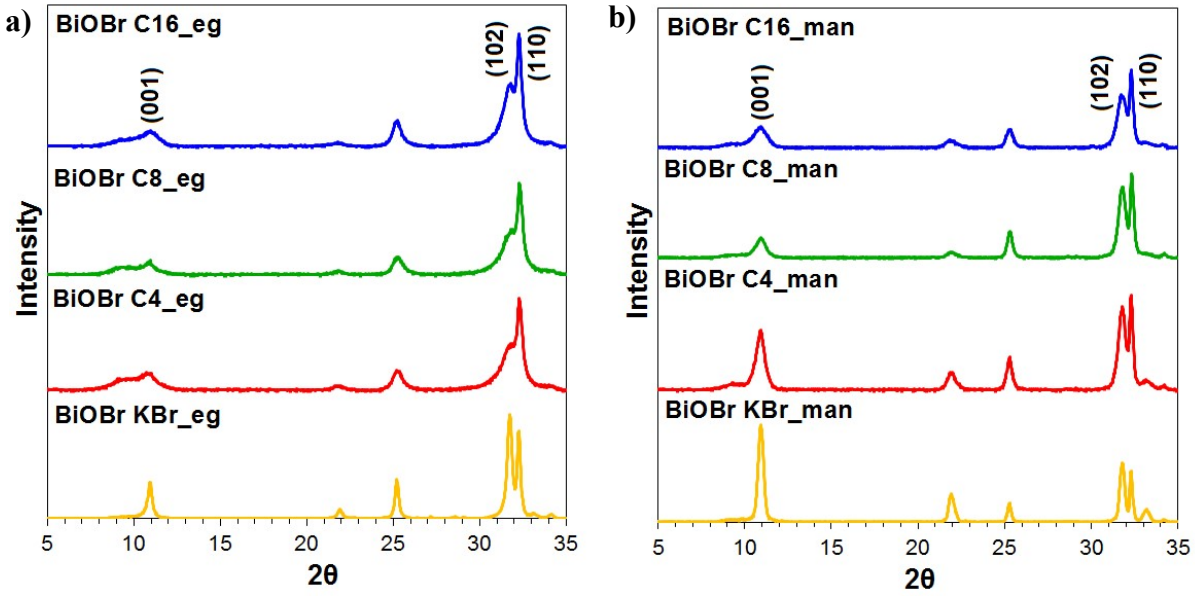

Figure S1. XRD diffractograms of BiOBr prepared in a) ethylene glycol and b) 0.1M mannitol at the selected 2θ range

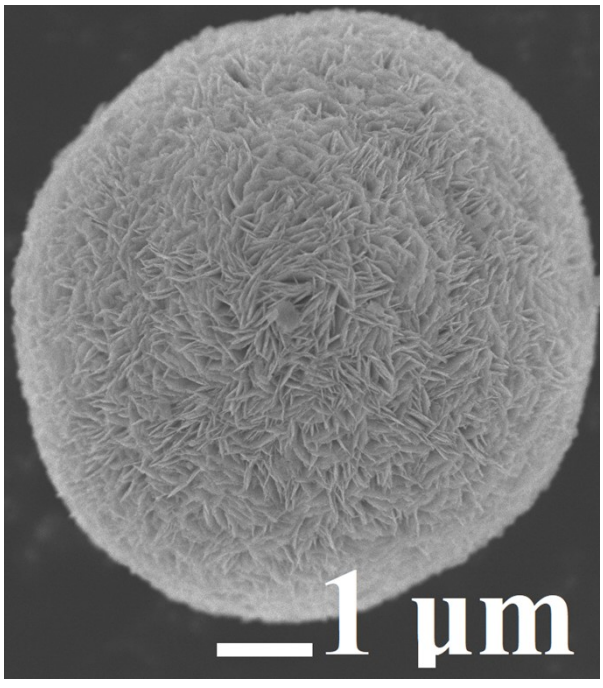

Figure S2. SEM image of BiOBr KBr_eg

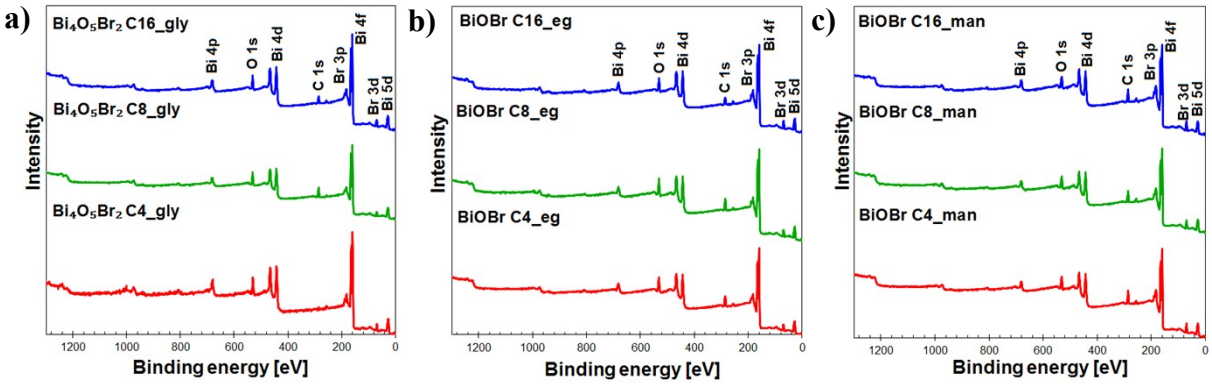

Figure S3. Survey spectra of photocatalysts prepared in a) glycerol, b) ethylene glycol and c) 0.1M mannitol

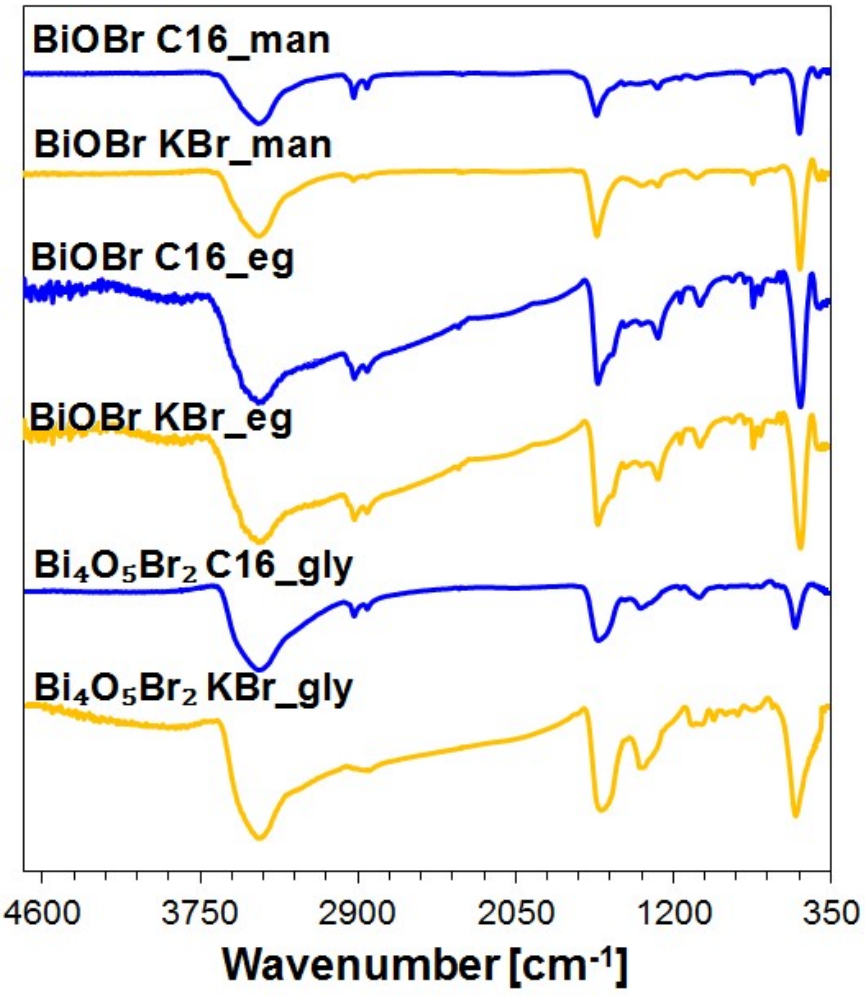

Figure S4. FT-IR spectra of selected photocatalysts

FT-IR spectra details

Figure S4 shows a series of Fourier-transform infrared (FTIR) spectra for selected $Bi_4O_5Br_2$ and BiOBr materials. The spectra of $Bi_4O_5Br_2$ KBr_gly and $Bi_4O_5Br_2$ C16_gly exhibit peaks at 525 cm^{-1}, 1400 cm^{-1}, 2850 cm^{-1} and 1630 cm^{-1}, 3450 cm^{-1}, which originating from Bi-O stretching vibrations, vibrations of C-H groups from adsorbed from air organic species, and surface-adsorbed water, respectively. The FTIR spectra of BiOBr samples had the same signals as those for $Bi_4O_5Br_2$ spectra.

Molecular dynamics calculation details

MD simulation sets were initially adjusting itself by changing their density through initial 50 ps of MD and then stabilized at constant levels of density. For the last 1 ns of each MD the resulting medium densities were 1.164 g/cm^3, 1.162 g/cm^3, 1.160 g/cm^3 and 1.166 g/cm^3 for C4M (C4mimBr), C8M (C8mimBr), C16M (C16mimBr) and POT (KBr) sets, respectively. Binding free energies and number of identified hydrogen bonds stabilized after 8 ns of MD, therefore for conclusive hydrogen bond analysis only last 1 ns of MD was considered. The total numbers of identified hydrogen bonds throughout last 1 ns of MD simulation was presented in Figure S5. The data plot lines were approximated with a Bézier curve to clearly expose the trends and their relative values.

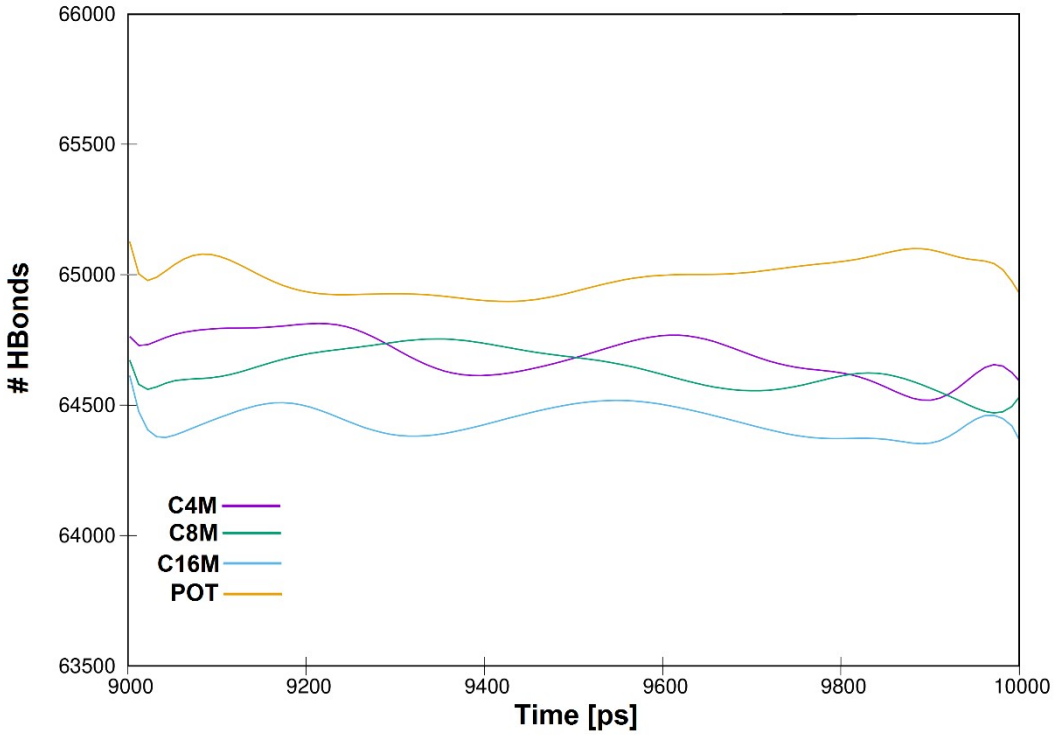

Figure S5. Averaged number of hydrogen bonds in last 1 ns of MD simulation.

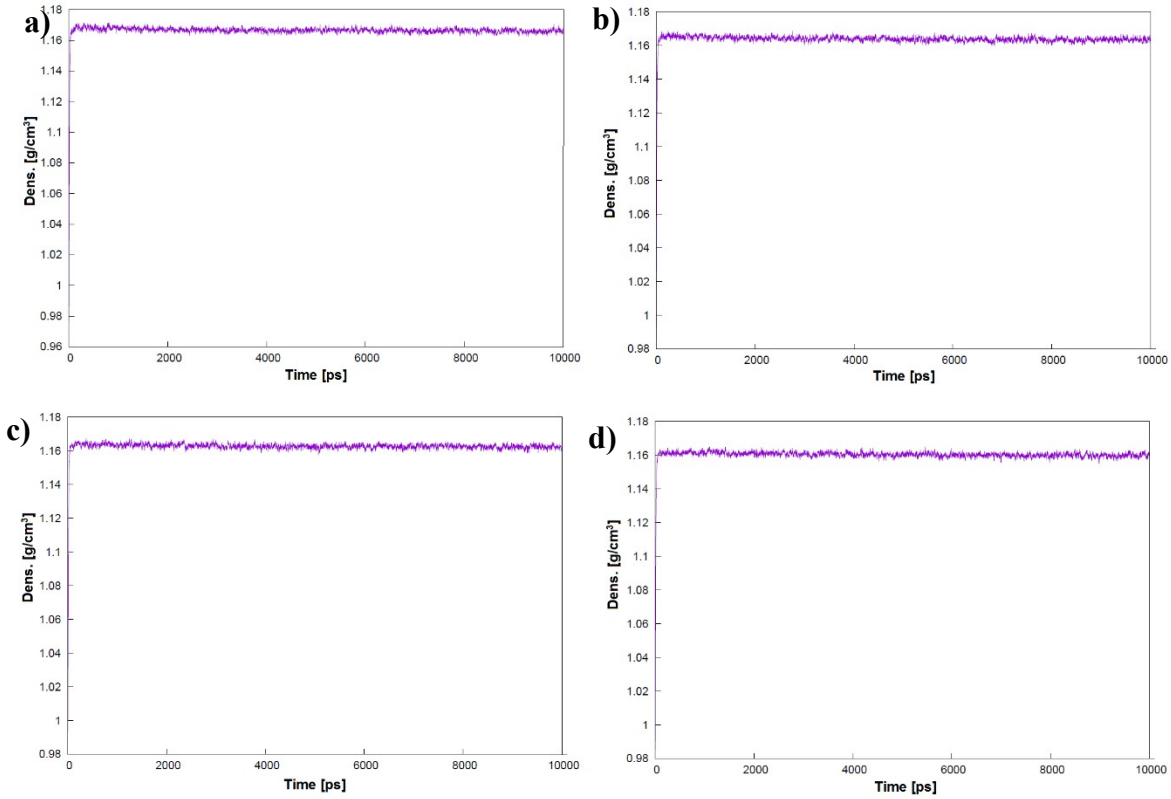

Figure S6. Medium density changes in MD of: a) POT, b) C4M, c) C8M and d) C16M sets.

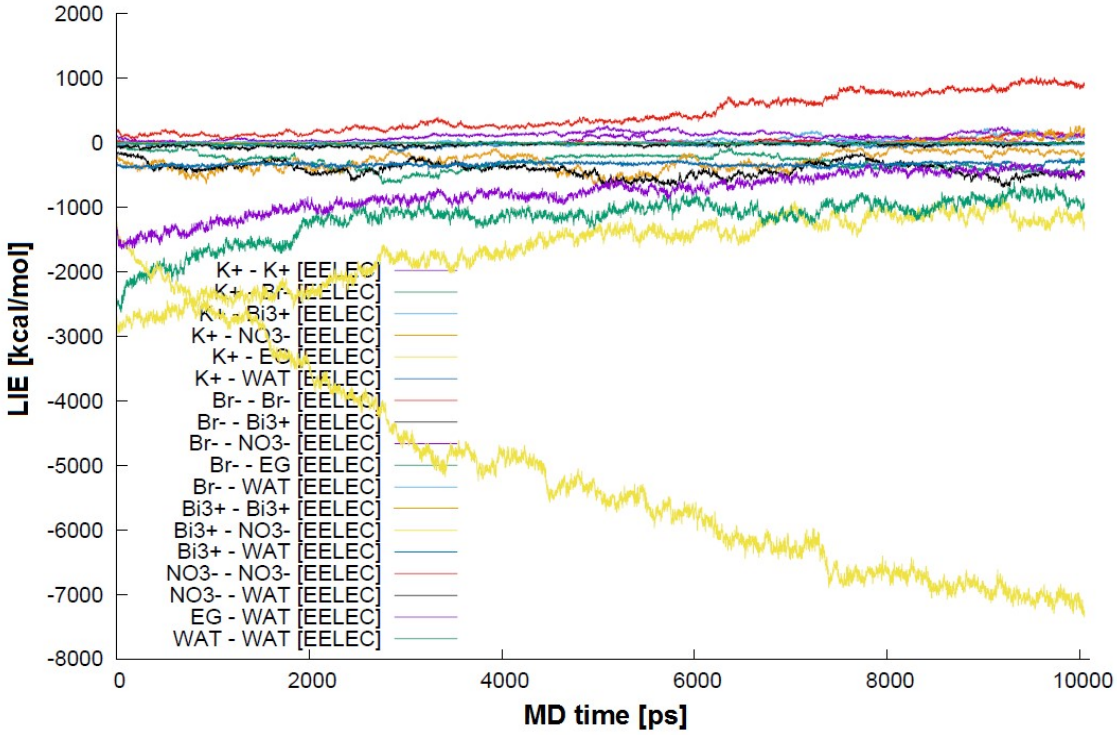

Figure S7. LIE changes in MD of POT set; electrostatic component

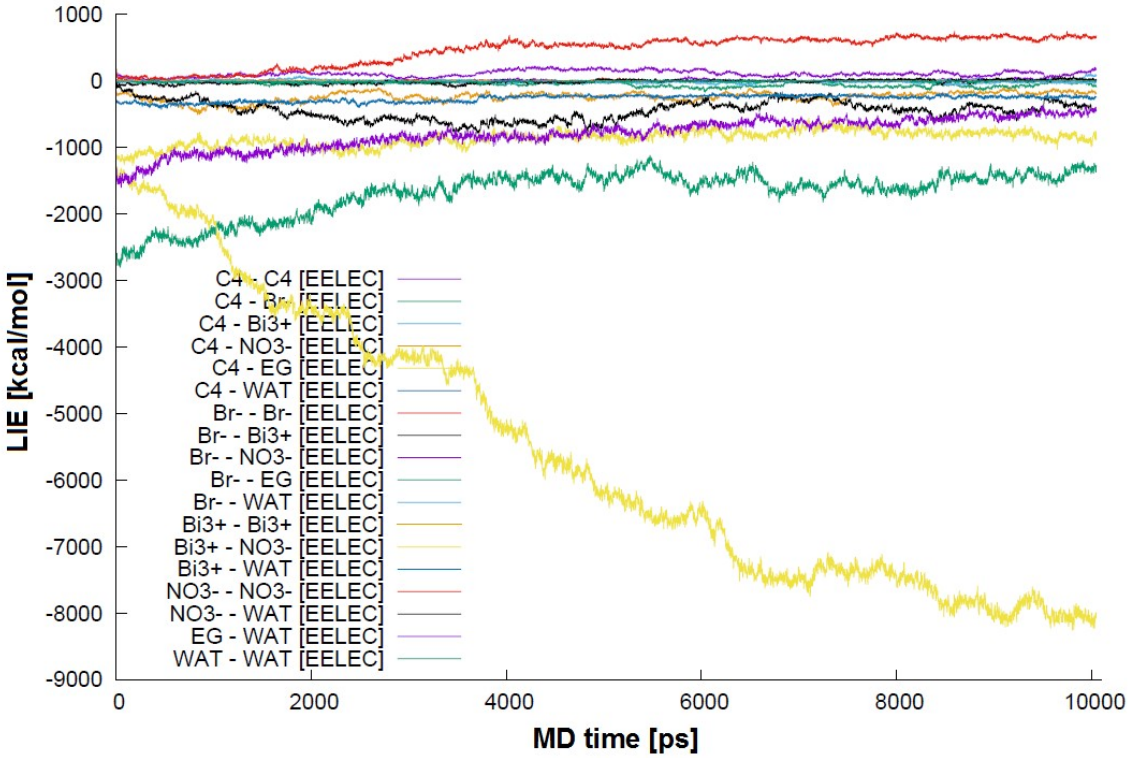

Figure S8. LIE changes in MD of C4M set; electrostatic component

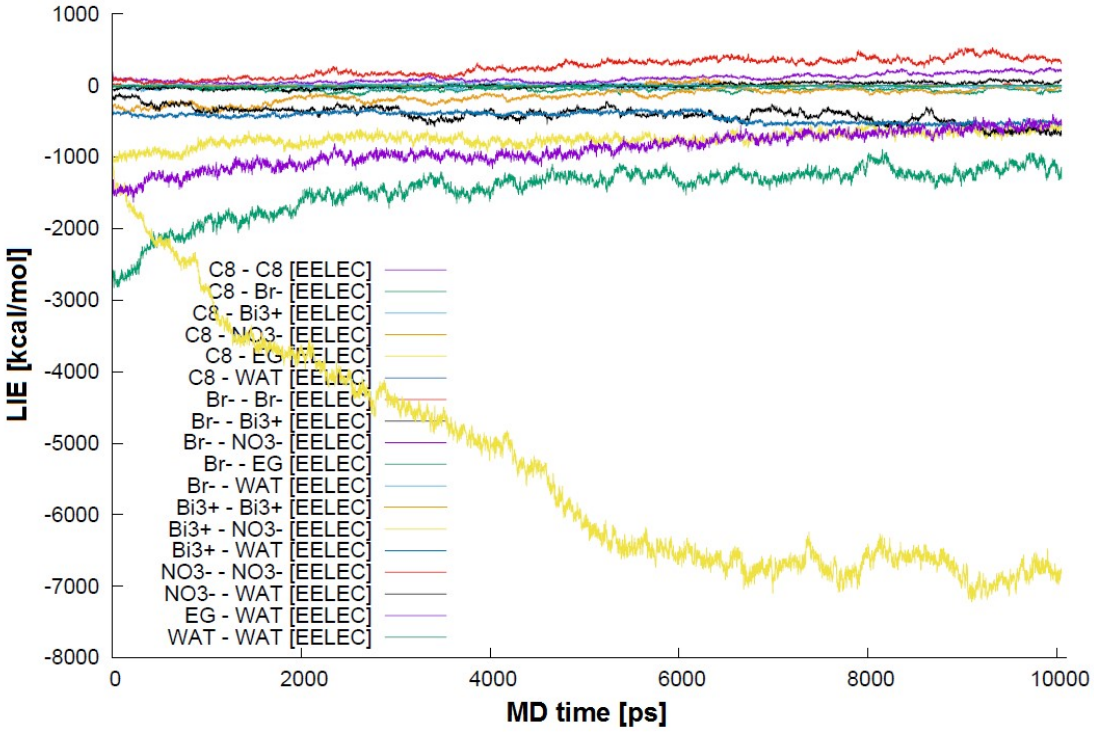

Figure S9. LIEchanges in MD of C8M set; electrostatic component

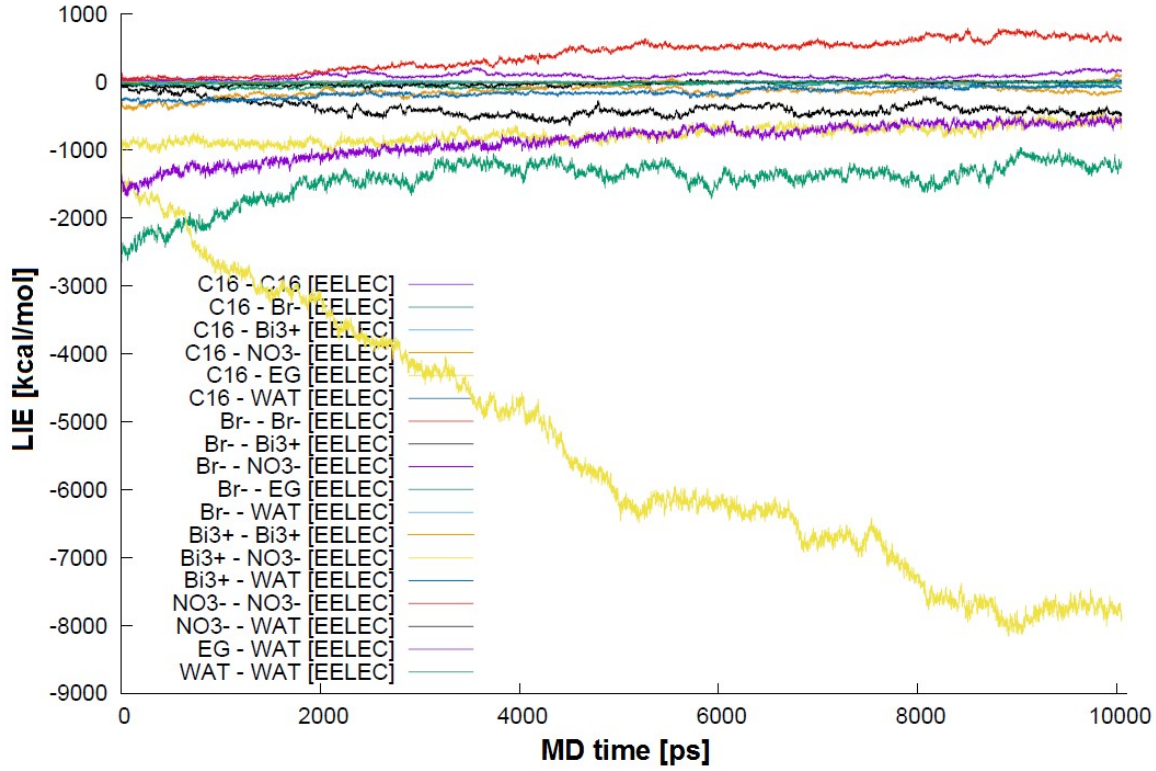

Figure S10. LIE changes in MD of C16M set; electrostatic component

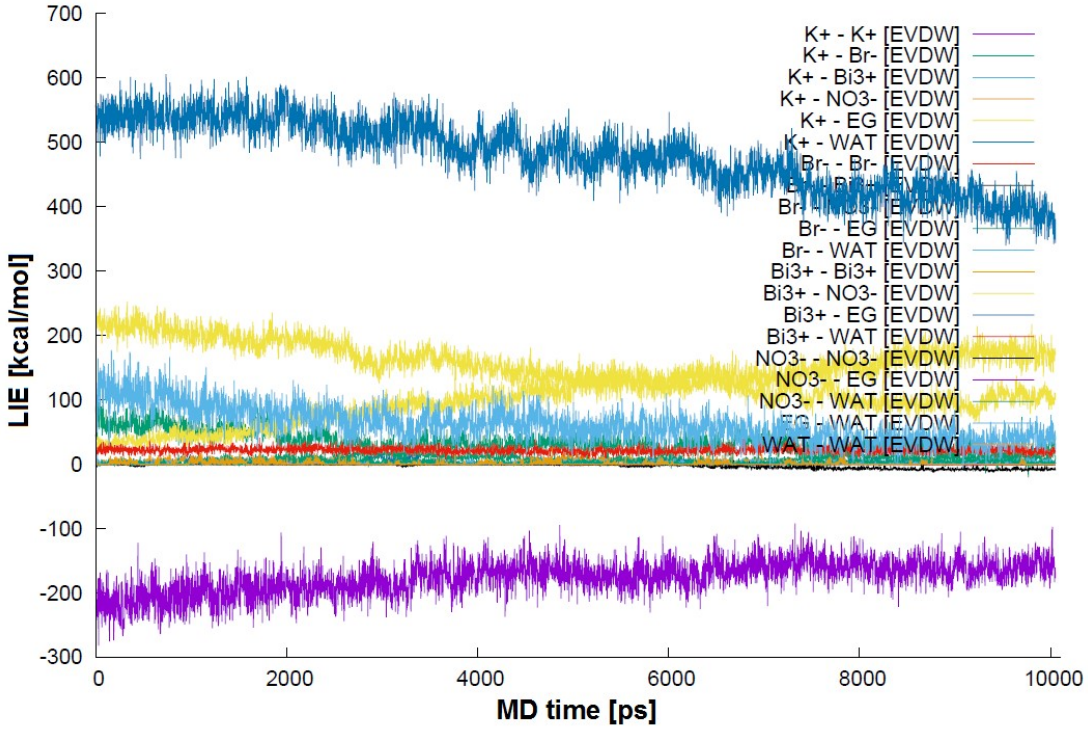

Figure S11. LIE changes in MD of POT set; van der Waals component

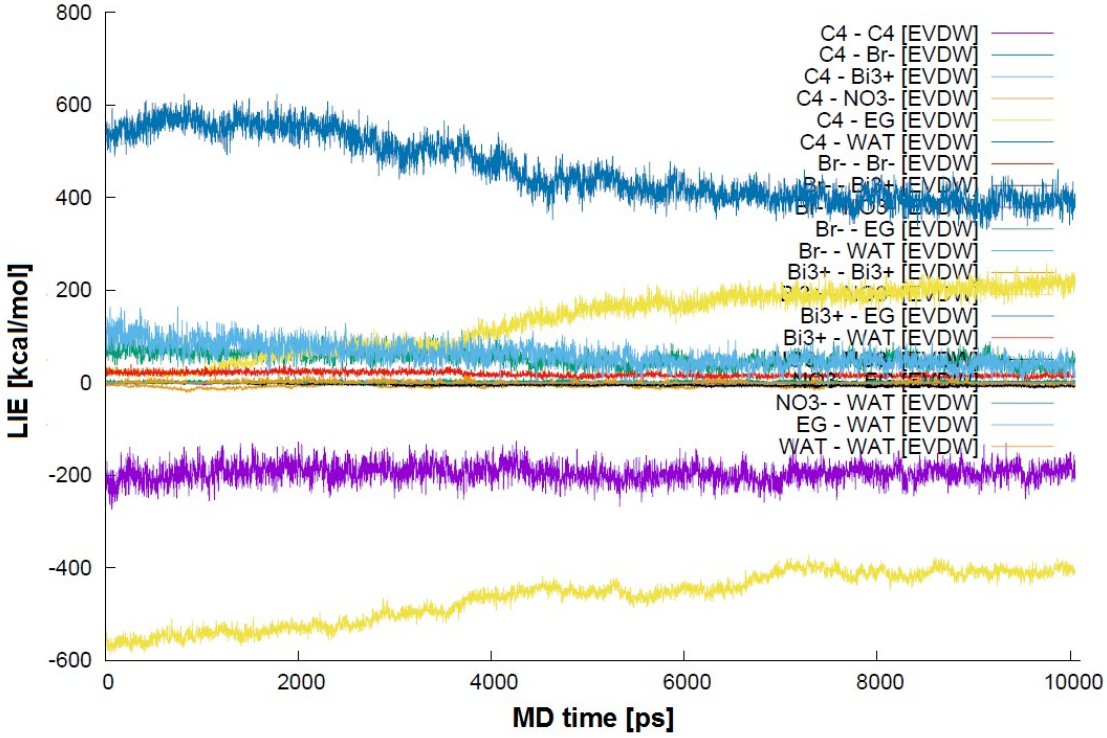

Figure S12. LIE changes in MD of C4M set; van der Waals component

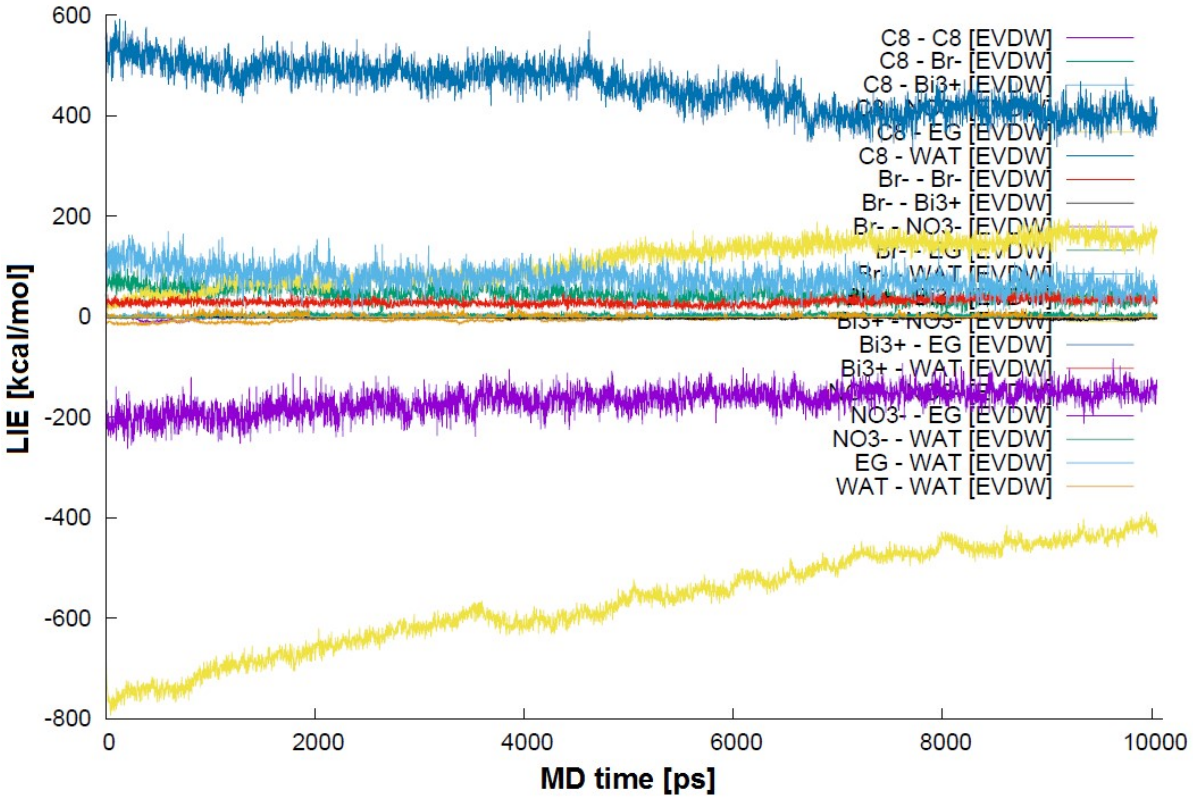

Figure S13. LIE changes in MD of C8M set; van der Waals component

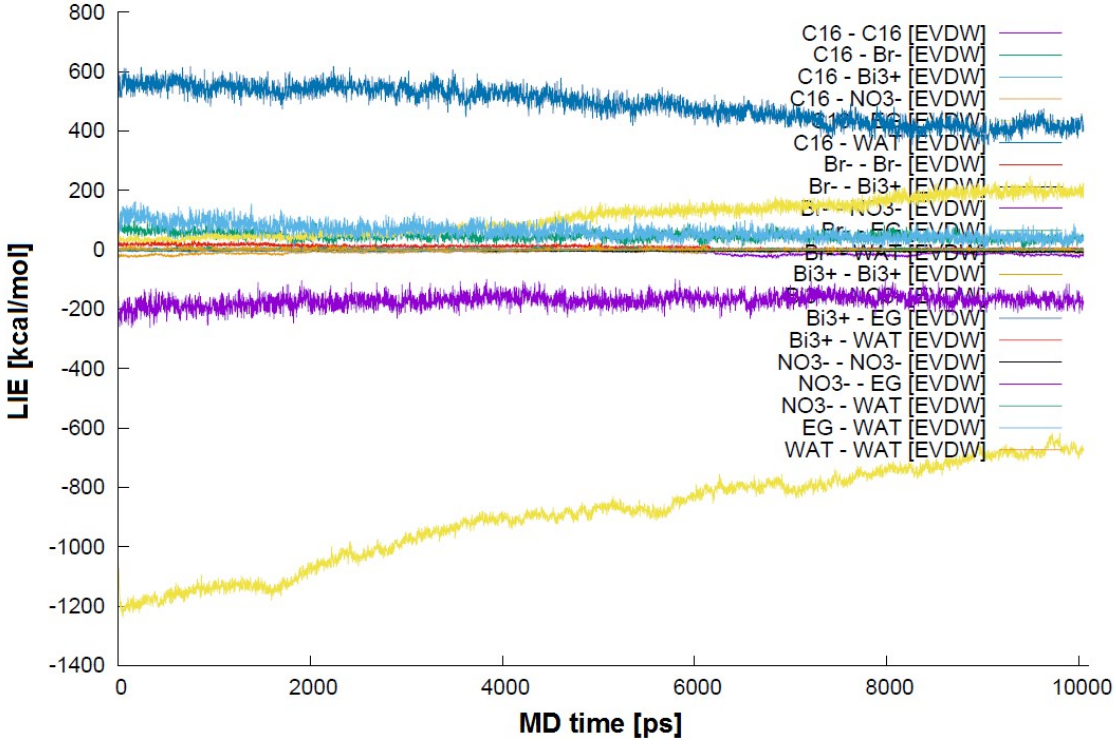

Figure S14. LIE changes in MD of C16M set; van der Waals component

Table S1. Electrostatic component of LIE energies averaged over last 1 ns of MD simulation of C4M set

	C4M	Br^-	Bi^{3+}	NO_3^-	EG	WAT
C4M	22.88	-49.82	19.00	-166.78	-825.68	-2.13
Br^-	-49.82	0.00	-400.77	118.60	-1,397.40	-18.55
Bi^{3+}	19.00	-400.77	0.00	-7,982.50	-11,125.76	-240.65
NO_3^-	-166.78	118.60	-7,982.50	656.18	-964.54	21.88
EG	-825.68	-1,397.40	-11,125.76	-964.54	-36,172.74	-491.54
WAT	-2.13	-18.55	-240.65	21.88	-491.54	-0.65

Table S2. Electrostatic component of LIE energies averaged over last 1 ns of MD simulation of C8M set

	C8M	Br^-	Bi^{3+}	NO_3^-	EG	WAT
C8M	0.55	-66.56	0.28	-38.14	-628.32	-1.56
Br^-	-66.56	1.51	-626.92	202.16	-1,136.11	-13.25
Bi^{3+}	0.28	-626.92	0.00	-6,885.60	-11,330.00	-524.46
NO_3^-	-38.14	202.16	-6,885.60	407.56	-795.23	52.21
EG	-628.32	-1,136.11	-11,330.00	-795.23	-36,729.07	-558.79
WAT	-1.56	-13.25	-524.46	52.21	-558.79	-1.79

Table S3. Electrostatic component of LIE energies averaged over last 1 ns of MD simulation of C16M set

	C16M	Br^-	Bi^{3+}	NO_3^-	EG	WAT
C16M	1.30	-57.06	19.18	-139.90	-577.75	-2.23
Br^-	-57.06	0.00	-442.98	144.59	-1,171.40	-9.88
Bi^{3+}	19.18	-442.98	15.21	-7,756.42	-11,729.74	-68.72
NO_3^-	-139.90	144.59	-7,756.42	672.37	-793.27	2.67
EG	-577.75	-1,171.40	-11,729.74	-793.27	-36,142.93	-597.19
WAT	-2.23	-9.88	-68.72	2.67	-597.19	-3.14

Table S4. Electrostatic component of LIE energies averaged over last 1 ns of MD simulation of POT set

	K^+	Br^-	Bi^{3+}	NO_3^-	EG	WAT
K^+	9.35	-389.70	125.96	-142.09	-1,139.70	-9.95
Br^-	-389.70	125.18	-519.03	138.39	-834.74	-26.96
Bi^{3+}	125.96	-519.03	92.32	-7,030.16	-11,412.03	-320.42
NO_3^-	-142.09	138.39	-7,030.16	909.17	-1,080.95	-16.94
EG	-1,139.70	-834.74	-11,412.03	-1,080.95	-35,780.12	-427.07
WAT	-9.95	-26.96	-320.42	-16.94	-427.07	-0.50

Table S5. Van der Waals component of LIE energies averaged over last 1 ns of MD simulation of C4M set

	C4M	Br^-	Bi^{3+}	NO_3^-	EG	WAT
C4M	-1.87	-0.52	-0.04	-4.71	-407.53	-0.30
Br^-	-0.52	0.00	-0.33	-0.29	40.84	1.13
Bi^{3+}	-0.04	-0.33	0.00	210.85	390.93	15.01
NO_3^-	-4.71	-0.29	210.85	210.85	-6.87	1.89
EG	-407.53	40.84	390.93	-191.37	-15,244.38	41.35
WAT	-0.30	1.13	15.01	1.89	41.35	-0.01

Table S6. Van der Waals component of LIE energies averaged over last 1 ns of MD simulation of C8M set

	C8M	Br^-	Bi^{3+}	NO_3^-	EG	WAT
C8M	-0.07	-0.94	0.00	-1.08	-430.85	-0.35
Br^-	-0.94	0.00	-0.76	-0.75	36.14	1.36
Bi^{3+}	0.00	-0.76	0.00	160.25	400.96	34.40
NO_3^-	-1.08	-0.75	160.25	160.25	-4.50	3.12
EG	-430.85	36.14	400.96	-147.73	-15,493.94	58.38
WAT	-0.35	1.36	34.40	3.12	58.38	0.25

Table S7. Van der Waals component of LIE energies averaged over last 1 ns of MD simulation of C16M set

	C16M	Br^-	Bi^{3+}	NO_3^-	EG	WAT
C16M	-15.60	-0.93	-0.11	-6.31	-676.64	-0.60
Br^-	-0.93	0.00	-0.53	-0.80	34.68	0.61
Bi^{3+}	-0.11	-0.53	0.00	196.55	415.54	3.03
NO_3^-	-6.31	-0.80	196.55	196.55	-5.98	1.42
EG	-676.64	34.68	415.54	-168.24	-15,343.52	40.18
WAT	-0.60	0.61	3.03	1.42	40.18	0.71

Table S8. Van der Waals component of LIE energies averaged over last 1 ns of MD simulation of POT set

	K^+	Br^-	Bi^{3+}	NO_3^-	EG	WAT
K^+	0.00	11.22	0.00	0.96	101.11	1.58
Br^-	11.22	-0.41	-0.53	-0.65	18.95	4.55
Bi^{3+}	0.00	-0.53	-0.01	173.11	398.09	21.10
NO_3^-	0.96	-0.65	173.11	173.11	-8.00	4.38
EG	101.11	18.95	398.09	-160.34	-15,314.35	39.39
WAT	1.58	4.55	21.10	4.38	39.39	0.10